Regulation of cell proliferation by nucleocytoplasmic dynamics of postnatal and embryonic exon-II-containing MBP isoforms

Ozgen, Hande; Kahya, Nicoletta; de Jonge, Jenny C.; Smith, Graham S. T.; Harauz, George; Hoekstra, Dick; Baron, Wia

Published in:
Biochimica et Biophysica Acta - Molecular Cell Research

DOI:
10.1016/j.bbamcr.2013.11.026

Biochimica et Biophysica Acta 1843 (2014) 517–530

Contents lists available at ScienceDirect

Biochimica et Biophysica Acta

journal homepage: www.elsevier.com/locate/bbamcr

Regulation of cell proliferation by nucleocytoplasmic dynamics of postnatal and embryonic exon-II-containing MBP isoforms

Hande Ozgen [a], Nicoletta Kahya [a], Jenny C. de Jonge [a], Graham S.T. Smith [b], George Harauz [b], Dick Hoekstra [a], Wia Baron [a,*]

[a] Department of Cell Biology, University of Groningen, University Medical Center Groningen, Antonius Deusinglaan 1, 9713 AV Groningen, The Netherlands
[b] Department of Molecular and Cellular Biology, University of Guelph, 50 Stone Road East, Guelph, ON N1G 2W1, Canada

ARTICLE INFO

Article history:
Received 4 September 2013
Received in revised form 26 November 2013
Accepted 29 November 2013
Available online 7 December 2013

Keywords:
Oligodendrocyte
MBP
Nucleocytoplasmic shuttling
Proliferation

ABSTRACT

The only known structural protein required for formation of myelin, produced by oligodendrocytes in the central nervous system, is myelin basic protein (MBP). This peripheral membrane protein has different developmentally-regulated isoforms, generated by alternative splicing. The isoforms are targeted to distinct subcellular locations, which is governed by the presence or absence of exon-II, although their functional expression is often less clear. Here, we investigated the role of exon-II-containing MBP isoforms and their link with cell proliferation. Live-cell imaging and FRAP analysis revealed a dynamic nucleocytoplasmic translocation of the exon-II-containing postnatal 21.5-kDa MBP isoform upon mitogenic modulation. Its nuclear export was blocked upon treatment with leptomycin B, an inhibitor of nuclear protein export. Next to the postnatal MBP isoforms, embryonic exon-II-containing MBP (e-MBP) is expressed in primary (immature) oligodendrocytes. The e-MBP isoform is exclusively present in OLN-93 cells, a rat-derived oligodendrocyte progenitor cell line, and interestingly, also in several non-CNS cell lines. As seen for postnatal MBPs, a similar nucleocytoplasmic translocation upon mitogenic modulation was observed for e-MBP. Thus, upon serum deprivation, e-MBP was excluded from the nucleus, whereas re-addition of serum re-established its nuclear localization, with a concomitant increase in proliferation. Knockdown of MBP by shRNA confirmed a role for e-MBP in OLN-93 proliferation, whereas the absence of e-MBP similarly reduced the proliferative capacity of non-CNS cell lines. Thus, exon-II-containing MBP isoforms may regulate cell proliferation via a mechanism that relies on their dynamic nuclear import and export, which is not restricted to the oligodendrocyte lineage.

1. Introduction

Oligodendrocytes are the myelinating cells of the central nervous system (CNS) with a distinct and carefully regulated proliferation and differentiation timeline. During their maturation, they synthesize myelin sheaths, which enwrap axons to provide fast nerve conduction and to ensure axonal integrity [1]. Myelin membranes contain various myelin specific proteins of which myelin basic protein (MBP) is the second most abundant one and, most importantly, the only known structural protein that is indispensable for CNS myelin formation [2–5].

Several MBP isoforms are present in oligodendrocytes and it has been well established that the MBP family is generated from a large, 11 exon-containing gene complex called Golli (gene in the oligodendrocyte lineage). Given the presence of two primary transcription starting sites, two subfamilies can be distinguished, i.e., classical MBPs, expressed by myelinating oligodendrocytes, and golli MBPs that are also expressed by many other cells [6–9]. From this large gene complex, the alternative splicing of the seven most downstream exons (denoted by Roman numerals I–VII) gives rise to a single MBP mRNA transcript [10], which is transcribed into different classical MBP isoforms, four of which, i.e., 21.5-, 18.5-, 17-, and 14-kDa, are predominantly expressed in rats. The 14- and 18.5-kDa isoforms lack exon-II and localize to compact myelin, whereas the exon-II-containing 17- and 21.5-kDa MBP isoforms localize predominantly to the nucleus, but also appear in the cytoplasm [11–13]. These classical postnatal MBP isoforms are synthesized in a developmentally-regulated manner. Thus, exon-II-positive MBP isoforms are expressed during early stages of myelination, whereas the expression of exon-II-negative MBP isoforms peaks in late myelination [14–16]. Interestingly, in addition to the classical MBP postnatal isoforms, embryonic isoforms also exist [17–18], including an exon-II-containing 16-kDa MBP isoform, the expression of which

Abbreviations: BSA, bovine serum albumin; BrdU, 5-Bromo-2′-deoxy-uridine; CDK, cyclin-dependent kinase; CNS, central nervous system; CRM1, chromosome region maintenance 1; C/N, cytoplasm / nucleus; FCS, fetal calf serum; FGF, fibroblast growth factor; FRAP, fluorescence recovery after photobleaching; e-MBP, embryonic myelin basic protein; GFP, green fluorescent protein; Golli, gene in the oligodendrocyte lineage; HD, high density; LD, low density; LMB, leptomycin B; mAb, monoclonal antibody; MBP, myelin basic protein; NES, nuclear export signal; N/C, nucleus / cytoplasm; N/M, nucleus / membrane OPC, oligodendrocyte progenitor cell; pAb, polyclonal antibody; PBS, phosphate-buffered saline; PDGF, platelet-derived growth factor; PFA, paraformaldehyde; PLL, poly-L-lysine; RFP, red fluorescent protein; RT, room temperature; SF, serum-free

* Corresponding author. Tel.: +31 503632737; fax: +31 503632728.
E-mail address: w.baron@umcg.nl (W. Baron).

0167-4889/$ – see front matter © 2013 Elsevier B.V. All rights reserved.
http://dx.doi.org/10.1016/j.bbamcr.2013.11.026

persists during the early postnatal phase in mice and rats [16–18], and which expression is not limited to the oligodendrocyte lineage [17].

Thus far, MBP-related research has largely focused on exon-II-negative MBP isoforms, whereas knowledge of the function of nuclear exon-II-positive MBP isoforms is rather scanty. Specifically, exon-II-negative isoforms play a role in myelin compaction, and also serve as 'molecular sieves' by selectively allowing access of only proteins with short cytoplasmic tails into myelin membranes [2,19–21]. In addition, these isoforms act in signaling, cytoskeleton polymerization and stabilization, and calcium–calmodulin binding [2,22–25]. In contrast, the exon-II-containing isoforms localize to the nucleus and cytoplasm when expressed in HeLa cells and oligodendrocytes [12,13], but the functional consequences of this distinct subcellular localization are still unresolved. However, as observed for other nuclear proteins, the localization of exon-II-containing MBP is affected by cell–cell contact [12], whereas nuclear translocation appears to be an active process, which is time, energy, and temperature dependent [12,26]. In terms of functioning, it is known that the 21.5-kDa MBP exon-II-containing isoform plays a role in calcium homeostasis in oligodendrocytes [23]. In addition, via the induction of a diffusible factor, 21.5-kDa MBP promotes proliferation of the immortalized N19-oligodendrocyte cell line, and enhances neurite outgrowth [27].

Here, we have investigated the role of the subcellular localization of postnatal and embryonic exon-II-positive MBP isoforms and their link with proliferation. Photobleaching (FRAP) and live-cell imaging techniques demonstrated a dynamic nucleocytoplasmic translocation of postnatal exon-II-containing 21.5-kDa MBP–RFP upon mitogenic modulation. Our findings further revealed that a 16-kDa exon-II-containing embryonic MBP isoform (e-MBP) is expressed in many cell lines, including non-myelinating cell lines, and like the postnatal 21.5-kDa MBP isoform, is involved in cell proliferation. Therefore, exon-II-containing MBP isoforms play a specific regulatory role not only in the early regulation of the myelin machinery, but in a more general context, also in (embryonic) cell proliferation.

2. Materials and methods

2.1. Cell culture

2.1.1. Primary oligodendrocytes

Primary oligodendrocyte cultures were generated from 1 to 3 day old Wistar rats as described [28]. Briefly, rats were decapitated, forebrains were collected, and a single cell suspension was obtained by mechanical and enzymatic (papain) digestion. Cells were cultured in DMEM (Gibco, Invitrogen, Paisley, Scotland) supplemented with 10% fetal calf serum (FCS, not heat-inactivated, Bodinco, Alkmaar, The Netherlands), L-glutamine (Invitrogen) and penicillin/streptomycin (P/S, Invitrogen) for 10–14 days on poly-L-lysine (PLL, 5 μg/mL, Sigma, St. Louis, MO)-coated tissue culture flasks (Nunc, Roskilde, Denmark). Oligodendrocyte progenitor cells (OPCs), growing on top of an astrocyte monolayer, were then isolated by a shake-off procedure, followed by differential adhesion. After shaking, OPCs were collected from the medium and for Western blot analysis plated on PLL-coated 10-cm dishes (Nunc, Naperville, IL) at a cell density of 10^6 cells/dish. The OPCs were cultured in SATO medium [28], containing PDGF-AA (10 ng/mL, Peprotech, Rocky Hill, NJ) and FGF-2 (10 ng/mL, Peprotech) for 2 days. Differentiation was induced by growth factor withdrawal and cells were allowed to differentiate for 3, 7, and 10 days in SATO medium supplemented with 0.5% FCS. Medium was refreshed twice a week.

2.1.2. Cell lines

The oligodendrocyte progenitor cell line OLN-93, a kind gift from Dr. Christiane Richter-Landsberg [29], was cultured in DMEM supplemented with L-glutamine, P/S and 10% FCS (heat-inactivated) under standard incubation conditions (humidified atmosphere, 7.5% CO_2, 37 °C). Experiments were performed at passage 25–36. For carrying out a proliferation assay and immunocytochemical analysis, the cells were cultured on 8-well chamber slides (Nunc), pre-coated with PLL at the indicated cell densities for 3 days. Cells were cultured in 10% FCS unless otherwise indicated. After 2 days in culture, cells were treated with 20 μM roscovitine (Sigma) or leptomycin B (LMB, 10 ng/mL, LC Laboratories, Woburn, MA) for 24 and 6 h, respectively. For Western blot analysis, cells were plated on PLL-coated 10-cm tissue culture dishes (Corning Costar, Lowell, MA). Cell densities were calculated according to the corresponding surface area of 8-well chambers. For fluorescence recovery after photobleaching (FRAP) and live-cell imaging, OLN-93 cells were plated on PLL-coated 2-well Labtek-II chambered coverglass (Nunc, 50,000 cells/well). After 24 h, cells were transfected with 21.5-kDa MBP–RFP [25] or RFP, using Lipofectamine™ 2000 Transfection Reagent (Invitrogen) as described in the manufacturer's instructions. Experiments were performed 24 h after transfection. HEK293, HeLa, and HepG2 cells were cultured as OLN-93 cells. For BrdU assays and e-MBP immunocytochemistry, cells were plated a day prior to the analyses on 13-mm glass cover slides in 24 well plates at a cell density of 25,000 (HeLa, HepG2) or 35,000 (HEK293) per well.

2.2. Rat brain tissue

Brain tissue of Wistar rats was homogenized, using a Wheaton homogenizer, in 1 mL of ice-cold TE buffer (10 mM Tris–HCl, 2 mM EDTA, 0.25 M sucrose) and a cocktail of protease inhibitors (Complete Mini, Roche Diagnostics, Mannheim, Germany). Samples were stored at −80 °C until further biochemical analysis.

2.3. Constructs and lentiviral transduction

The generation of the plasmid coding for 21.5-kDa MBP–RFP has been described previously (pERFP-C1-rmMBP-21.5-UTR [23]). The plasmid coding for RFP was pERFP-C1. Lentiviral-mediated knockdown of gene expression was performed using the pHR′trip-PGK-eGFP-WPRE-H1 vector. For this purpose, the vector was modified to allow for insertion of different short hairpins. In short, the pHR′trip-PGK-eGFP-WPRE-H1 vector was amplified with two opposing primers containing either the recognition sequence for *Asc*I (5′-CGTGGCGCGCCATCTGTGGTCTC ATACAGAACTT-3′) or *Sbf*I (5′-CGTCCTGCAGGGGAAAAGCTTATGAATTC GGC-3′) and self-ligated (restriction sites underlined). The PCR amplification was performed using *Pfu* turbo DNA polymerase (Stratagene, La Jolla, CA). Short hairpin sequences cloned into the modified vector had the following topology: 5′-acaaGGCGCGCC(N19-23)actcgaga(N19-23c)gtttttCCTGCAGGacaa-3′ (*Asc*I and *Sbf*I restriction sites in capital letters). Ordered DNA oligonucleotides (Biolegio, Nijmegen, The Netherlands) were primed with a reverse primer (5′-TTGTGCCTGC AGGAAAAA-3′) and filled in using Phi29 DNA polymerase (New England Biolabs, Beverly, MA). Ligation was performed using 1 μL of hairpin DNA and 150 ng of digested modified pHR′trip-PGK-eGFP-WPRE-H1. The target sequence for MBP, directed against the interface of exon-III and exon-IV, was: 5′-acaaaGGCGCGCCA GCAGAGGA CCCAAGATGAAACTCGAGATTCATCTTGGGTCCTCTGCGTTTTTCCTGCA GGcacaa-3′. Lentiviral particles were produced as described [30]. Cells were exposed to two times diluted lentiviruses containing MBP shRNA, for 16 h in the presence of 4 μg/mL hexadimethrine bromide (polybrene; Sigma). Concomitant expression of GFP confirmed shRNA transduction. Analyses were performed 10–15 days after transduction.

2.4. RT-PCR

Total RNA was isolated on day 3 using the InviTrap Spin Cell RNA Mini Kit (Invitek, Stratec, Berlin, Germany). The RNA yield and purity were quantified spectrophotometrically by measuring A260 and A280 absorbances in a Nano-Drop ND-Spectrophotometer (V3.1.0, Thermo

Scientific, Wilmington, NC). From total RNA (1 μg), cDNA synthesis was performed in the presence of oligo(dT) 12–18 and dNTPs (Gibco) with superscript II reverse transcriptase (Roche Diagnostic, Almere, Netherlands) according to the manufacturer's instructions. From total cDNA, the embryonic DNA band was generated by using a forward primer against embryonic exon [17], 5′-GGGAGGACAACACCTTCAAA-3′ and a reverse primer against MBP–exon-II, 5′-GGCATGAGAAGGCA GAGG-3′. Primers were designed and purchased from Biolegio (Nijmegen, The Netherlands). The reaction conditions were 1 cycle of 5 min at 94 °C, followed by 55 cycles of 30 s at 94 °C, 30 s at 55 °C, 1 min at 72 °C, and 1 cycle of 7 min at 72 °C. The samples were run on a 2% agarose gel.

2.5. Subcellular fractionation

After three washes with phosphate-buffered saline (PBS), cells were scraped in 500 μL subcellular fractionation buffer (250 mM sucrose, 20 nM HEPES pH 7.4, 10 mM KCl, 1.5 mM $MgCl_2$, 1 mM EDTA, 1 mM EGTA, 1 mM DTT and protease inhibitor cocktail), and collected in a 1.5-mL Eppendorf tube. The lysates were passed 20 times through a 25G needle, using a 1-mL syringe, and cooled for 20 min on ice. The nuclear fraction was pelleted at 720 *g* for 5 min at 4 °C. The supernatant was collected. The nuclear pellet was dissolved in 500 μL fractionation buffer, dispersed with a pipette, and passed 10 times through a 25G needle, and centrifuged at 720 *g* for 10 min. The supernatant was collected and the nuclear pellet was washed 5 times with fractionation buffer. In parallel, to separate the membrane fraction (pellet) from the cytoplasmic fraction (supernatant), the collected supernatants were centrifuged at 10,000 *g* for 30 min at 4 °C. The cytoplasmic fraction was precipitated with trichloroacetic acid [31]. The nuclear, membrane, and cytoplasmic pellets were dissolved in equal amounts of TNE lysis buffer (50 mM Tris–HCl, 5 mM EDTA, 150 mM NaCl, 1% Triton X-100, and protease inhibitor cocktail), and subjected to Western blot analysis.

2.6. Immunocytochemistry

Cells were fixed with 2% paraformaldehyde (PFA, Merck) for 15 min at room temperature (RT) followed by incubation for 15 min with 4% PFA at RT. Cells were washed three times with PBS, and blocked and permeabilized with 0.1% Triton X-100 in 4% bovine serum albumin (BSA) for 30 min at RT. Cells were incubated with primary antibodies diluted in 4% BSA for 1 h at RT. Primary antibodies were monoclonal rat anti-MBP antibody (1:10, Millipore, Billerica, MA), and polyclonal anti-GFP (1:00, Molecular Probes, Invitrogen). After washing three times with PBS, cells were incubated with Alexa- (1:500, Invitrogen) or Cy3- (1:400, Jackson ImmunoResearch, West Baltimore Pike, PA) conjugated secondary antibodies diluted in 4% BSA for 30 min at RT, followed by washing three times with PBS. During incubation with the secondary antibody, DRAQ5™ (1:500, Bistatus Limited, Leicestershire, UK) was also included to visualize the nuclei. Cells were mounted in DAKO mounting medium. Images were acquired by confocal microscopy, using a Leica SP2 AOBS CLSM (Leica Microsystems, Heidelberg, Germany) equipped with an argon laser (488 nm), 2 He/Ne lasers (543 and 633 nm, respectively) and with Leica confocal software. A 63×/1.25 oil immersion objective was used for 2-channel scanning. The Cy3/Alexa 546 and Alexa 633 signals were recorded sequentially in the green and red channels, respectively. The percentage of cells that expressed MBP in their nucleus was quantified by determining the ratio of cells with nuclear MBP over the total cell number. At least 10 fields, each containing more than 30 cells, were counted in three independent experiments.

2.7. BrdU incorporation assay

Cell proliferation was determined by a 5-Bromo-2′-deoxy-uridine (BrdU)-incorporation assay (Roche), according to the manufacturer's instructions with slight modifications. Three days after plating, cells were incubated with 10 μM BrdU for 8 h (OLN-93) or 16 h (HEK293, HeLa) at 37 °C prior to fixation. The cells were washed three times with PBS and fixed with ice cold 95% ethanol–5% acetic acid for 15 min at RT. Subsequently, the cells were incubated with mouse monoclonal IgG antibody against BrdU (1:15) in a humidified chamber for 30 min at 37 °C, followed by three washes with PBS and an incubation with secondary antibody, anti-mouse Ig-fluorescein (1:15) for 30 min at 37 °C. During incubation with the secondary antibody, DRAQ5™ was also included to stain the nuclei. After washing three times with PBS, cells were examined by fluorescence microscopy as described above. The percentage of proliferating cells was quantified by determining the ratio of BrdU-positive cells over DRAQ5™- or GFP-positive cells. When the proliferation assay was carried out on the same sample as e-MBP immunocytochemistry, the cells were first subjected to e-MBP-immunocytochemistry (see above). The percentage of proliferating cells that express e-MBP in the nucleus was quantified by determining the ratio of cells with nuclear e-MBP over the total number of proliferating cells. At least 10 fields, each containing more than 40 cells, were counted in three independent experiments.

2.8. Live-cell imaging

At 24 h after transfection, cells were subjected to live-cell imaging for 3 or 6 h at 37 °C under an atmosphere of 5% CO_2. All measurements were done in the presence of cycloheximide (50 μg/mL, Sigma), which was added 1 h before the onset of the experiment. The Z-stacks with 0.5 μm optical serial sections were acquired every 10 min using a Spinning Disk Leica DM IRE2 confocal laser scanning microscope (Leica Microsystems, Heidelberg, Germany), equipped with a 63×/1.3 glycerol immersion objective, and Argon (457 nm, 476 nm, 488 nm, 514 nm), and Krypton (568 nm, 647 nm) lasers. Under these conditions, and given the low laser power used, bleaching hardly occurred, if at all. Images were recorded with a Stanford Photonics XR/Mega-10I (intensified)-CCD camera using intuitive InVivo (Media Cybernetics) software with imaging format 1024 × 1024 pixels. In order to avoid any movement of the cell in the z direction, the z-stacks were merged to one picture using Imaris (Bitplane AG, Switzerland).

2.9. FRAP analysis

At 24 h after transfection, the cells were subjected to FRAP analysis as described in [32] using a Zeiss 780 NLO confocal laser scanning microscope (Carl Zeiss MicroImaging GmbH, Jena, Germany), equipped with a 63×/1.3 glycerol immersion objective in an acquisition mode 256 × 256 frame size, 2.55-μs pixel dwell time, 390.98-ms scan time without averaging. Briefly, 10 pre-bleach images were taken. Bleaching was performed with a DPSS-laser (561 nm) at 100% laser power. To monitor nuclear import, the entire nucleus was bleached, whereas for determination of nuclear export, the cytoplasm was bleached. For bleaching of the nucleus, 13 iterations with 100.85-μs pixel dwell time, and for bleaching the cytoplasm, 6 iterations for MBP–RFP and 9 iterations for RFP with 50.85-μs pixel dwell time were used, resulting in 90% bleaching of the nucleus and 70–80% bleaching of the cytoplasm. Post-bleach images were taken in 4 sets. The first set consisted of 30 frames, taken at an interval of 0.4 s (fastest); the second of 30 frames with 1.2-s intervals, the third of 30 frames at 5-s time intervals, and the remainder was taken at 10-s intervals. The images were acquired at 1% laser power. Importantly, upon continuous bleaching of dye-loaded plastic at one particular region, our system bleached up to a depth of 9 μm in the z direction (data not shown). Accordingly, since OLN-93 cells form a layer with a thickness of 5 μm, our system is capable of readily bleaching the entire nucleus or cytoplasm. The fluorescence intensities of the bleached area (nucleus or cytoplasm) and non-bleached area (cytoplasm or nucleus) were analyzed by ZEN software (Zeiss). In addition, an area where no cells were present was recorded,

which was considered as the background signal. The background signal was very low, however for the accuracy of our calculations, the signal was subtracted from the fluorescence intensities of the bleached and non-bleached areas. For determination of the nuclear import rate, the ratio of fluorescence intensity of nucleus to cytoplasm was calculated. The pre-bleach ratio was set to 100%, and the other values were calculated accordingly. For determining the nuclear export rate, the ratio of fluorescence intensity of cytoplasm to nucleus was calculated. Import rates of 1500 s for 21.5-kDa MBP–RFP and 600 s for RFP, and export rates of 1400 s for 21.5-kDa MBP–RFP and 600 s for RFP were analyzed, using a one-phase association curve in GraphPad Prism 5. To compare the rates at the different conditions, half-lives were plotted separately and compared, using a one way ANOVA followed by a Newman–Keuls posttest.

2.10. Western blot analysis

Cells were scraped in PBS and centrifuged at 9000 *g* for 10 min at RT. Cell pellets were lysed in TNE-lysis buffer. Protein concentrations were determined by a BioRad DC protein assay (Bio-Rad Laboratories, Hercules, CA), using BSA as standard. For the total cell lysate, equal amounts of protein (total cell lysates) or volume (subcellular fractionation) were mixed with reducing sample buffer, heated for 5 min at 95 °C, and applied onto 15% SDS-polyacrylamide gels. Proteins were transferred to a nitrocellulose membrane using a wet blotting system (Bio-Rad). The membranes were rinsed with PBS and incubated for 1 h in blocking buffer (Odyssey blocking buffer (Li-Cor Biosciences, Lincoln, NE), diluted with an equal volume of PBS) at RT. After blocking, the membranes were incubated overnight with primary antibodies diluted in blocking buffer containing 0.1% Tween-20. Primary antibodies used were monoclonal rat anti-MBP (1:100), polyclonal rabbit anti-MBP (1:1000, Dakocytomation, Carpinteria, CA), polyclonal guinea pig anti-exon-II (1:1000, a kind gift from Dr. Liliana Pedraza, Montréal, Canada [12]), monoclonal mouse anti-histone H3 antibody (Abcam, Cambridge, UK), monoclonal anti-mouse NCAM 140/180 (Sigma), and monoclonal mouse anti-β-actin (1:1000, Sigma) diluted in blocking buffer. The membranes probed with polyclonal guinea pig anti-exon-II were incubated next with a goat anti-guinea pig IgG linker antibody (1:1000, Jackson ImmunoResearch). The membranes were washed three times with PBS containing 0.05% Tween-20 (PBS-T) and incubated for 1 h with appropriate IRDye-conjugated secondary antibodies (Li-Cor Biosciences) at RT. After incubation, membranes were washed three times with PBS-T. Signals were detected using the Odyssey Infrared Imaging System (Li-Cor Biosciences). The protein bands were quantified by the imaging software ImageJ.

2.11. Statistics

Data (mean ± standard deviation (SD)) for both immunocytochemistry and Western blots were analyzed from at least three independent experiments. Statistical significance was calculated by Student's t-test for comparison between two means and by one-way ANOVA followed by Newman–Keuls posttest to compare more than two means in GraphPad Prism 5. p-Values <0.05, <0.01, and <0.001 are considered statistically significant (*, **, and ***, respectively).

3. Results

3.1. The localization of 21.5-kDa MBP in OLN-93 cells changes upon mitogenic modulation

To investigate the potential role of nucleus-localized exon-II-containing MBP isoforms as mitogenic modulators, we employed an oligodendrocyte-derived cell line, OLN-93. These cells represent an established model for the oligodendrocyte progenitor cells, and importantly, like many other oligodendroglial cell lines, they do not express postnatal classical MBP isoforms [23,29]. Therefore, OLN-93 cells may serve as a convenient model to study the function of exon-II-positive MBP isoforms without potential interference of exon-II-negative MBP isoforms, as their presence downregulates the expression of exon-II-containing MBP isoforms.

To assess whether 21.5-kDa MBP regulates proliferation in OLN-93 cells, we transfected the cells with RFP-tagged 21.5-kDa MBP and RFP alone, and subsequently examined their proliferation with a BrdU-incorporation assay. Transfection with 21.5-kDa MBP–RFP significantly increased total OLN-93 proliferation as compared to RFP-transfected cells (Fig. 1A, B). Remarkably, not only the proliferation of the transfected cells was increased, but also the proliferation of the cells that did not express 21.5-kDa MBP (Fig. 1A), suggesting that a secreted diffusible factor might modulate proliferation, as has been suggested recently [27].

To determine whether the known distinct cytoplasmic versus nuclear localization of 21.5-kDa MBP, and hence nucleocytoplasmic translocation, might be linked to proliferation, we next examined the intracellular localization of 21.5-kDa MBP–RFP upon mitogenic modulation. When cultured in 10% FCS-containing medium, i.e., a condition where cells are highly proliferative, the OLN-93 cells displayed a primarily nuclear localization of the 21.5-kDa MBP–RFP (Fig. 1C, D). In contrast, upon serum deprivation, i.e., a condition that inhibits proliferation, the nuclear localization of 21.5-kDa MBP–RFP decreased by approx. 30%. However, re-addition of serum at least partially re-established the nuclear localization of the 21.5-kDa isoform (SF + Recovery; Fig. 1C, D). Interestingly, upon treatment with leptomycin B (LMB), an unsaturated, branched-chain fatty acid that blocks nuclear export of many proteins [33,34], the 21.5-kDa MBP–RFP remained trapped in the nucleus at serum-free conditions (SF + LMB; Fig. 1C, D).

To examine in further detail whether a regulated nucleocytoplasmic translocation upon mitogenic modulation relies upon active shuttling of the MBP-isoform between the nucleus and cytoplasm, we exploited the fluorescence properties of the RFP-labeled 21.5-kDa isoform. As revealed by live-cell imaging, when 24 h after transfection MBP–RFP labeled cells were subsequently cultured in serum-free medium, the labeled protein rapidly disappeared from the nucleus within a time interval of approx. 2 h, after which the process further proceeded until nuclear localization could be barely detected after 6 h (cf., Fig. 1E, 10% FCS versus SF). However, when LMB was included into the serum-free medium, nuclear export of 21.5-kDa MBP–RFP was effectively prevented (Fig. 1E, SF + LMB). Re-addition of serum-containing media to the cells at either condition, which re-established the proliferative state of the cells, simultaneously led to a relatively fast 'recovery' of nucleus-localized MBP–RFP, which occurred as fast as within approx. 30 min after addition of serum-containing medium (Fig. 1E, SF + Recovery). To exclude de novo synthesis of transporters and MBP under the various conditions, all the experiments were performed in the presence of the protein synthesis inhibitor cycloheximide. Importantly, the nucleocytoplasmic shuttling of 21.5-kDa MBP–RFP was not an RFP-induced artifact, as the localization behavior of RFP alone was not altered upon mitogenic modulation (Supplementary Fig. 1). In this context, it is also relevant to note that RFP is considered the most appropriate control, since exon-II-negative MBP isoforms will not enter the nucleus. Hence, our findings indicate that the postnatal 21.5-kDa exon-II containing MBP isoform displays a considerable dynamics as reflected by its exit and entry into the nucleus, thereby closely correlating with cell proliferation of OLN-93 cells.

3.2. 21.5-kDa MBP actively shuttles in OLN-93 cells between the nucleus and cytoplasm upon mitogenic modulation

To more precisely determine the dynamics and nuclear export and import rates of the exon-II-containing 21.5-kDa MBP–RFP in live cells, we next performed photobleaching experiments (FRAP) under similar

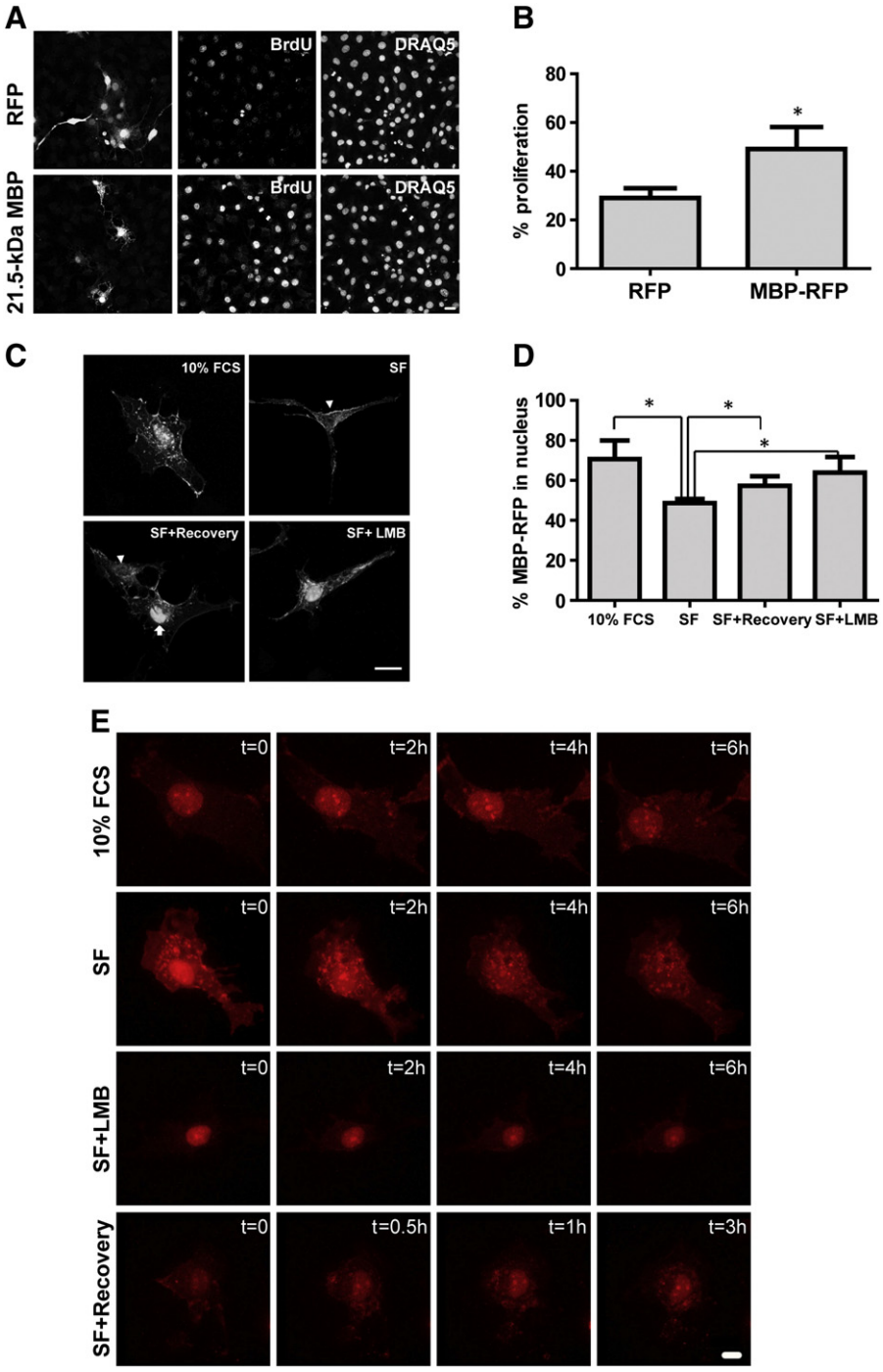

Fig. 1. The localization of 21.5-kDa MBP–RFP changes upon mitogenic modulation. OLN-93 cells were transiently transfected with 21.5-kDa MBP–RFP or RFP and treated as indicated. (A, B) At 24 h after transfection, cell proliferation was determined using a BrdU incorporation assay. The percentage of proliferative cells, i.e., BrdU-positive, of total, i.e., DRAQ5-positive cells was determined. Scale bar is 25 μM. Note that transfection with 21.5-kDa MBP–RFP significantly increases proliferation as compared to transfection with RFP alone (t-test, $^*p < 0.05$). (C, D) Cells were either fixed 24 h after transfection (10% FCS), or cultured in serum-free medium in the absence (SF) or presence of 10 ng/mL leptomycin B (SF + LMB). After 6 h, cells were fixed or allowed to recover in normal culture medium supplemented with 20% FCS (SF + Recovery) for 3 h. Localization of 21.5-kDa MBP–RFP at the indicated condition is shown in panel C. Given the low transfection efficiency, representative single cells of 3 independent experiments are shown. Scale bar is 20 μm. At the indicated conditions, the percentage of cells with nuclear 21.5-kDa MBP–RFP expression, relative to the total, DRAQ5-positive cells was examined (panel D). Note that upon inhibition of cell proliferation, 21.5-kDa MBP–RFP preferentially localizes to the cytoplasm in the absence of LMB, but not in the presence of LMB, whereas in control and during recovery, i.e., at proliferating conditions, 21.5-kDa MBP–RFP shows a more pronounced nuclear localization. The graphs were plotted as mean + SD and statistical analysis was performed by GraphPad Prism 5 (one-way ANOVA followed by the Newman–Keuls posttest; $^*p < 0.05$). (E) 24 h after transfection, the localization of 21.5-kDa MBP–RFP was recorded in live cells for 6 h in 10% FCS, and in serum-free medium in the absence (SF) or presence of 10 ng/mL leptomycin B (SF + LMB). Alternatively, cells were kept for 6 h in serum-free medium, after which the cell images were recorded for 3 h in medium supplemented with 20% (SF + Recovery). Z-stacks with 0.5 μm optical sections were acquired every 10 min. 3D image analysis was performed by IMARIS software. All measurements were performed in the presence of 50 μg/mL cycloheximide to inhibit de novo protein synthesis. Scale bar is 10 μm. Note that 21.5-kDa MBP–RFP remained in the nucleus in medium containing 10% FCS, whereas in serum-free medium 21.5-kDa MBP–RFP translocates to the cytoplasm in the absence, but not in the presence of LMB. During recovery, 21.5-kDa MBP–RFP translocates to the nucleus.

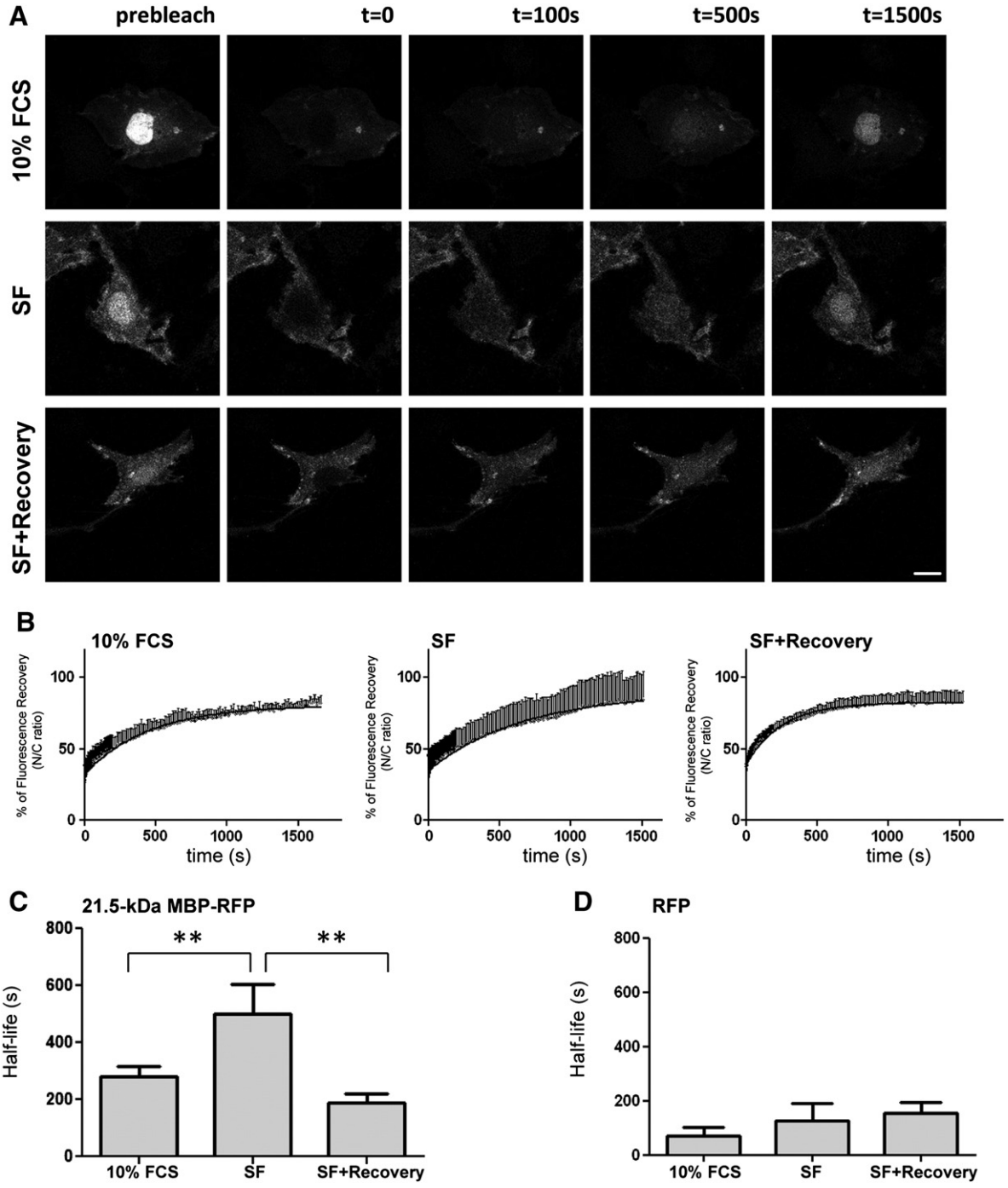

Fig. 2. Nuclear import rate of 21.5-kDa MBP–RFP changes upon mitogenic modulation. (A) OLN-93 cells were transiently transfected with 21.5-kDa MBP–RFP or RFP (control). At 24 h after transfection, cells were subjected to FRAP analysis in 10% FCS, or prior to FRAP analysis pretreated with serum-free medium for 6 h (SF), or allowed to recover from incubation for 6 h in serum-free medium (3 h in 20% FCS, SF + Recovery). Representative confocal images of cells positive for 21.5-kDa MBP–RFP, before and after bleaching of the nucleus at all conditions, are shown. Images were acquired with 1% laser power, and during bleaching 100% laser power was used. Scale bar is 10 μm. (B–D) Quantitative analysis of the nuclear import rate of (A). The ratio of fluorescence intensities of nucleus to cytoplasm (N/C) was set to 100% (after subtraction of background) and the ratio after bleaching was calculated accordingly. The results are plotted on the graph and fitted with a one-phase association curve using GraphPad Prism 5 (B). The half-life was calculated for each condition over a 1500-s time period for the 21.5-kDa MBP–RFP (C), and for 600 s for the RFP (D). Note that the nuclear import rate was significantly lower in serum-free medium and significantly higher during recovery, when compared to the rate obtained in the presence of 10% FCS for 21.5-kDa MBP–RFP (but not for RFP). For each condition, 8–10 cells were measured at once and this procedure was repeated at least three times. The graphs were plotted as mean + SD and statistical analysis was performed using GraphPad Prism 5 (one-way ANOVA followed by the Newman–Keuls posttest $^{**}p < 0.01$).

conditions as the live-cell imaging experiments. FRAP is a powerful technique to study the dynamic behavior of proteins, while it provides detailed insight into the kinetics of the protein of interest [35–38]. To measure nuclear import rates, the 21.5-kDa MBP–RFP-fluorescence, present in the nucleus, was bleached up to 90% (Fig. 2A), and the rate of the recovery of fluorescence intensity was recorded for up to 1500 s, i.e., when it reached its equilibrium. Compared to other nucleocytoplasmic shuttling proteins, the fluorescence recovery rate of 21.5-kDa MBP–RFP was relatively slow as compared to β-catenin, Lgs, and VDBRB1 [38–40], but similar to STAT3 [36]. Fluorescence recovery in the nucleus was calculated and shown as the nuclear to cytoplasmic ratio (N/C ratio) in one-phase association curves (Fig. 2B). Interestingly, the nuclear import rate of MBP–RFP, as reflected by its shorter half-life, was significantly faster in medium containing 10% FCS than in serum-

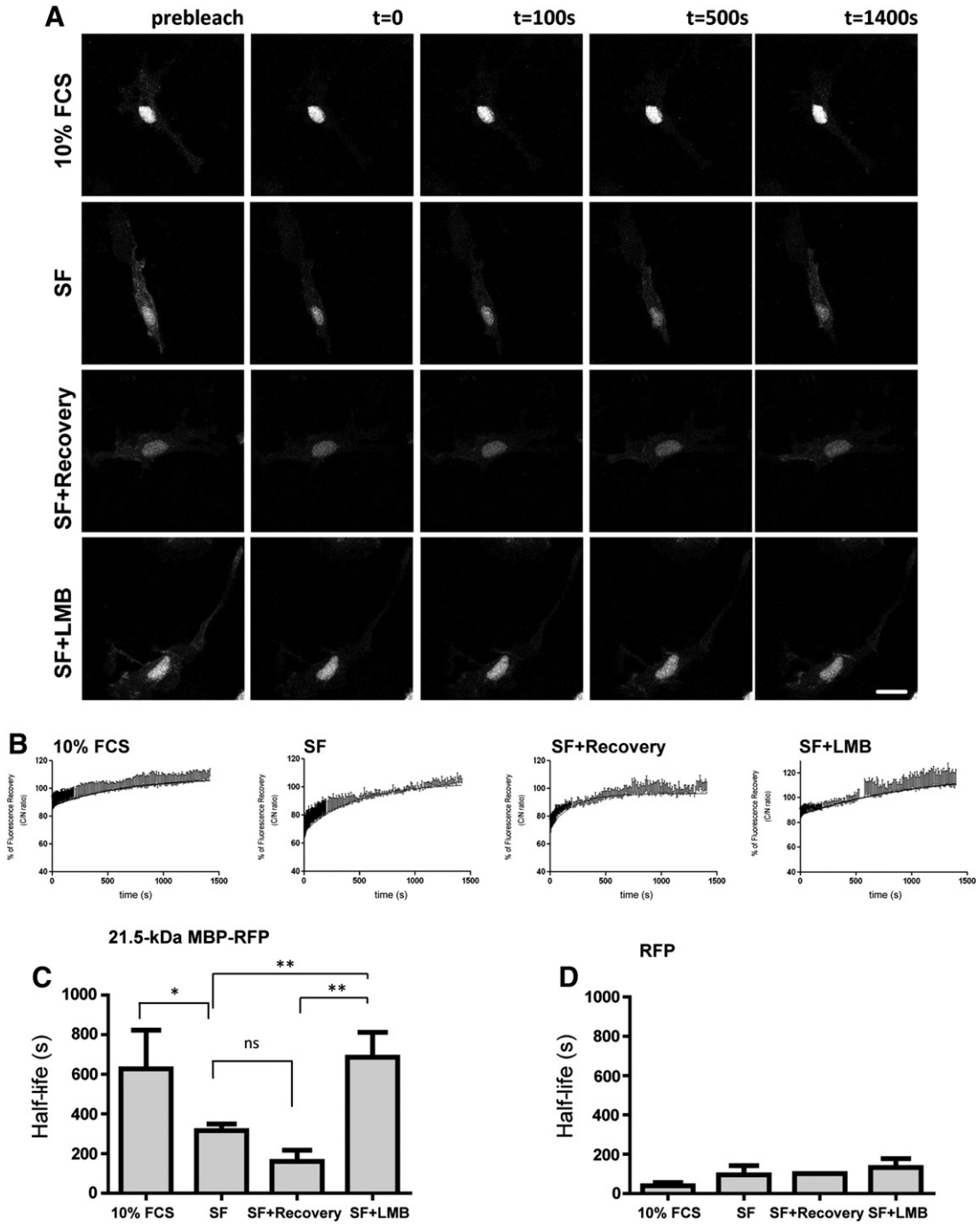

Fig. 3. Nuclear export rate of 21.5-kDa MBP–RFP changes upon mitogenic modulation. (A) OLN-93 cells were transiently transfected with 21.5-kDa MBP–RFP or RFP (control). At 24 h after transfection, cells were subjected to FRAP analysis in 10% FCS, or prior to FRAP analysis pretreated with serum-free medium for 6 h in the absence (SF) or presence of leptomycin B (SF + LMB), or allowed to recover from incubation for 6 h in serum-free medium (3 h in 20% FCS, SF + Recovery). Representative confocal images of cells positive for 21.5-kDa MBP–RFP before and after bleaching of the cytoplasm at all conditions are shown. Images were acquired with 1% laser power, and during bleaching 100% laser power was used. Scale bar is 10 μm. (B–D) Quantitative analysis of the nuclear export rate of (A). The ratio of fluorescence intensities of cytoplasm to nucleus (C/N) was set to 100% (after subtraction of background) and the ratio after bleaching was calculated accordingly. The results are plotted on the graph and fitted with a one-phase association curve using GraphPad Prism 5 (B). The half-life was calculated for each condition over a 1500-s time period for the 21.5-kDa MBP–RFP (C), and for 600 s for the RFP (D). Note that the nuclear export rate is significantly higher in serum-free medium, when compared to the rate obtained in the presence of 10% FCS for 21.5-kDaMBP–RFP (but not for RFP). For each condition, 8–10 cells were measured at once, and this procedure was repeated at least 3 times. The graphs were plotted as mean + SD and statistical analysis was performed using GraphPad Prism 5 (one-way ANOVA followed by the Newman–Keuls posttest $^{*}p < 0.05$, $^{**}p < 0.01$).

free conditions (Fig. 2C). The nuclear import half-life decreased again upon re-addition of 10% FCS to a rate similar to that as determined before serum-depletion (Recovery). Notably, mitogenic modulation did not affect the nuclear import rate of RFP (Fig. 2D, Supplementary Fig. 2).

Next, we determined the nuclear export kinetics of 21.5-kDa MBP–RFP upon mitogenic modulation. For that purpose, the 21.5-kDa MBP–RFP fluorescence of the cytoplasm was bleached up to 70–80% (Fig. 3A). As for determination of the import rates, the fluorescence

recovery rate, i.e., export from the nucleus to the cytoplasm (C/N ratio), was monitored until it reached equilibrium after approx. 1400 s (Fig. 3B). Like the nuclear import rate, the nuclear export rate was slower, when compared to other proteins mentioned above [38–40], but also proteins such as STAT3 with similar export rates have been reported [36]. Analysis of the half-lives revealed that the nuclear export rate of 21.5-kDa MBP–RFP was significantly slower in 10% FCS than in serum-free conditions. However, when OLN-93 cells were simultaneously treated with LMB, thereby inhibiting CRM1-dependent nuclear protein export, the nuclear export rate became substantially slower as reflected by a longer half-life, confirming the live-cell imaging results, and further suggesting that the nuclear export of 21.5-kDa MBP–RFP is nuclear export signal (NES)-dependent. Surprisingly, the nuclear export rate of 21.5-kDa MBP–RFP, 3 h after mitogenic recovery, was not decreased, given a short half-life value comparable to the half-life of 21.5-kDa MBP–RFP in serum-free medium. This result may suggest that additional factors, such as post-translational modification or other proteins, might regulate MBP nuclear export. As for nuclear import, FRAP analysis for RFP revealed that the nuclear export rates of RFP were not dependent on mitogenic modulation (Fig. 3D, Supplementary Fig. 3), indicating MBP specificity. Importantly, these findings show in addition that at 10% FCS, i.e., in mitogenic conditions, the import rate of 21.5-kDa MBP–RFP exceeds the rate of export (300 s vs. 600 s respectively), meaning that 21.5-kDa MBP–RFP will be located in the nucleus at cell proliferation. Hence, FRAP analysis supports active shuttling of 21.5-kDa MBP–RFP between the nucleus and cytoplasm in OLN-93 cells upon mitogenic modulation. As noted above, OLN-93 cells do not express postnatal MBP isoforms, but it has been suggested that there is an embryonic MBP isoform, which is expressed prior to the expression of postnatal MBP isoforms [29]. Given the mitogenic modulation of cells by an exon-II driven shuttling of MBP, it was therefore of particular interest to subsequently examine whether this embryonic MBP isoform harbors exon-II, and may similarly act as a regulator of cell proliferation.

3.3. OLN-93 cells express embryonic exon-II containing MBP, localizing in the nucleus and cytoplasm

As shown in Fig. 4 (arrows), using a monoclonal and polyclonal antibody that both recognize all MBP isoforms, OLN-93 cells abundantly express an MBP isoform with an apparent molecular mass of 16 kDa. This isoform did not correspond to any of the classical postnatal MBP isoforms, i.e., 21.5-, 18.5-, 17- and 14-kDa, which were visualized on the same immunoblot using myelin extracts of adult brain. In addition, a weak immunoreactive band was detected at approx. 13 kDa (Fig. 4A, arrowhead). Western blot analysis with an antibody directed against MBP–exon-II [12] revealed that both 16- and 13-kDa MBP isoforms in OLN-93 cells are reactive, indicating that these isoforms contain exon-II (Fig. 4A). The anti-exon-II antibody only recognizes the exon-II-containing MBP isoforms in rat myelin (17- and 21.5-kDa), confirming its specificity. Thus far, an exon-II-containing 13-kDa MBP isoform has not been described. Interestingly, an isoform with a molecular mass of 16 kDa has been detected during mouse and rat CNS development, and was identified as an embryonic MBP (e-MBP) isoform [16,17,41].

To verify whether the 16-kDa MBP isoform in OLN-93 cells has an embryonic origin, we next analyzed the expression of e-MBP at the mRNA level. Using a primer set that recognizes the embryonic exon [17] and exon-II, RT-PCR analysis revealed the presence of e-MBP

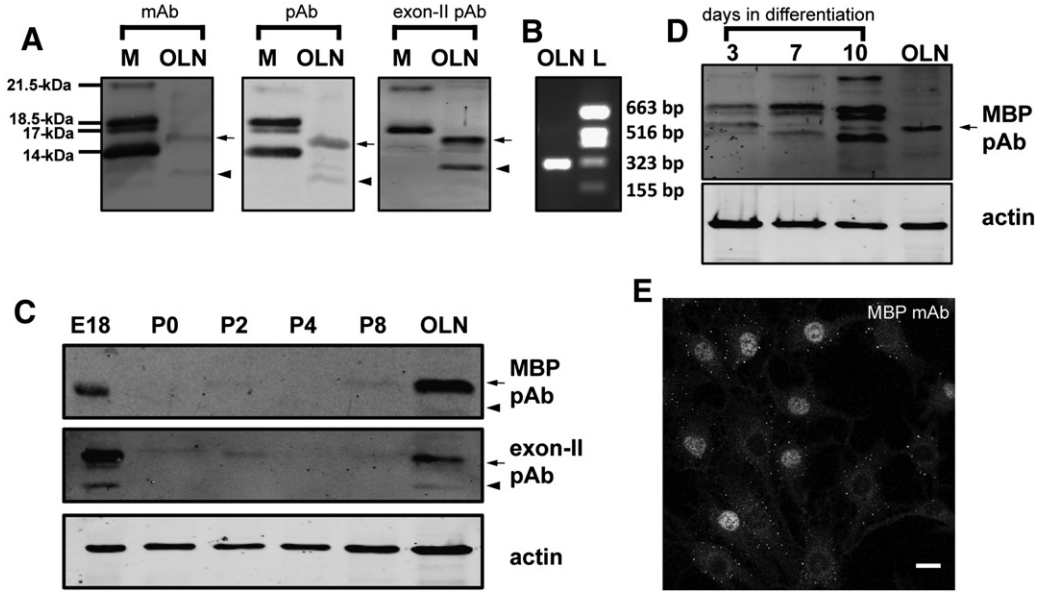

Fig. 4. OLN-93 cells express 16-kDa e-MBP, localizing in the nucleus and cytoplasm. (A) Equal amounts of protein of total cell lysates of OLN-93 (OLN, 50 μg) and myelin extracts of adult rat brain (M, 7 μg) were subjected to Western blot analysis. The expression of MBP was visualized using two different antibodies directed against all MBP isoforms (monoclonal and polyclonal antibodies), and a polyclonal antibody directed against MBP-specific exon-II [12]. Note that the molecular mass of the most prominent MBP isoform present in OLN-93 cells is around 16 kDa (arrow), whereas the classical MBP isoforms present in myelin appear at 14, 17, 18.5, and 21.5 kDa. In addition, an exon-II-reactive band at 13 kDa was present in OLN-93 cells (arrowhead). (B) Total RNA was isolated from OLN-93 cells and RT-PCR was performed using a specific set of primers to detect e-MBP, i.e., forward primer against embryonic exon and reverse primer against exon-II. The "L" designates the kb ladder. (C) Equal amounts of protein (20 μg), obtained from the indicated embryonic (E) and postnatal (P) total rat brain lysates were subjected to Western blot analysis. The expression of MBP was characterized using two different anti-MBP antibodies, i.e., directed against exon-II or against all MBP isoforms (polyclonal). The expression of MBP isoforms is compared to the isoform present in OLN-93 cells (50 μg). Note that the 16-kDa MBP isoform present in OLN-93 cells is abundantly expressed at embryonic day 18 (arrow). (D) Primary rat oligodendrocytes were collected at the indicated days after initiating differentiation. Equal amounts of protein (20 μg) were subjected to Western blot analysis for MBP expression. Note that the 16-kDa MBP isoform (arrow) is expressed by cultured oligodendrocytes even at 10 days after initiating differentiation; however, it is more enriched during early differentiation, i.e., 3 days after initiating differentiation. Notably, given the abundant presence of exon-II-negative MBP isoforms in myelin, the blots in (A) are shown at a lower intensity as in (C) and (D). (E) OLN-93 cells, 3 days in culture, were fixed and stained with anti-MBP monoclonal antibody. A representative confocal image of three independent experiments is shown. Note that MBP localizes both to the nucleus (bright fluorescence) and to the cytoplasm (punctate appearance). Scale bar is 20 μm.

mRNA (Fig. 4B). To obtain further support for the presence of e-MBP in OLN-93 cells, the expression of MBP isoforms during early rat brain development was compared to the expression of MBP isoforms in OLN-93 lysates. As shown in Fig. 4C, prominent expression of exon-II-containing MBP isoforms with the same molecular masses as present in OLN-93 cells was apparent in the embryonic stage (E18). These variants, however, readily disappeared within the early phase (i.e., within 72–96 h) of the postnatal stage. Furthermore, the 16-kDa e-MBP band was also detected in prenatal rat brain (Fig. 4C, arrow) and in primary rat oligodendrocytes at different maturation stages after initiating differentiation (Fig. 4D, arrow). Interestingly, the 16-kDa e-MBP was more prominently expressed early (i.e., 3 days) after initiating differentiation, than at later stages (7 and 10 days), whereas the exon-II specificity of this isoform was confirmed with an anti-exon-II antibody (data not shown).

As indicated above, given that e-MBP contains exon-II, we therefore next examined whether e-MBP and postnatal exon-II-positive MBP isoforms have similar subcellular localizations. Immunocytochemical studies revealed that e-MBP, similarly as the postnatal exon-II-positive 21.5-kDa MBP–RFP in OLN-93 cells, and postnatal exon-II MBP isoforms in oligodendrocytes (not shown; [12,26,42]), displayed a nucleocytoplasmic distribution pattern (Fig. 4E). Remarkably, cytoplasmic expression appeared as dots, consistent with a previous study [29]. Unfortunately, the anti-exon-II antibody is not suitable for immunocytochemistry. Since the 16-kDa e-MBP represents by far the major MBP fraction (Fig. 4A), we assume that the distinctive localization in either the cytoplasm, nucleus, or both reflects the distribution of this particular isoform.

3.4. The localization of embryonic MBP correlates with cell proliferation

As previously shown in HeLa cells, cell density is one of the factors that affects the intracellular distribution of postnatal exon-II-positive MBP isoforms. Thus, when cells are plated at high cell density, the percentage of nuclear MBP localization decreases as compared to low-density cultures [12]. To determine whether e-MBP behaves similarly as classical postnatal exon-II positive MBP isoforms [12], OLN-93 cells were plated at a low and high cell density and subsequently cultured for 3 days. At low density, approx. 50% of the cells showed a nuclear localization for e-MBP, whereas in high-density cultures, e-MBP was largely excluded from the nucleus, i.e., the percentage of cells with nuclear e-MBP was reduced to approx. 15% (Fig. 5A, B, LD and HD, respectively). Importantly, it should be noted that the overall expression levels of e-MBP were not affected by cell density (Fig. 5C), suggesting a genuine shift in intracellular e-MBP distribution.

To obtain further support for such a cell density dependent shift, subcellular fractionation was carried out. To this end, three subcellular fractions, i.e., a nuclear, membrane, and cytoplasmic fraction were isolated from equal volumes of cell lysates obtained from low- and high-density cultures. Consistent with its physical nature as a peripheral membrane-bound protein, e-MBP was present in either the nuclear or membrane fraction, whereas it was completely absent from the cytoplasmic fraction (Fig. 5D). To assess the purity of the different fractions, NCAM 140 was used a membrane marker, and histone 3 as a marker for the nuclear fraction. Thus, after appropriate corrections for fraction purity, the nucleus to membrane ratio was consistently decreased in high-density cultures (Fig. 5D), in agreement with the immunocytochemical data (Fig. 5A, B). Together, these data indicate that cell density does not alter the overall expression levels of e-MBP, but does affect translocation of the protein from the nucleus to the cytoplasm. Previous studies have provided evidence that cell density controls cell proliferation, i.e., cells proliferate faster in low-density cultures than in high-density cultures [43,44]. We therefore next examined whether, as for 21.5-kDa MBP, there might be a direct link between cell proliferation and e-MBP translocation.

To examine OLN-93 cell proliferation as a function of cell density, a BrdU incorporation assay was performed. As shown in Fig. 5F, proliferation was slightly, but significantly, decreased at high cell density relative to low cell density. Concomitantly, the majority of the proliferating cells also showed a nuclear staining for e-MBP at low-density cultures (Fig. 5E, G). In contrast, at high cell density, only a minor fraction of the proliferating cells harbor nuclear e-MBP, suggesting an uncoupling of cell proliferation and nuclear e-MBP expression upon cell–cell contact. Of note, e-MBP might regulate rather than trigger proliferation, as 55% of the cells that had nuclear e-MBP at high cell density cultures did incorporate BrdU during an 8 h pulse, whereas only 12% of nuclear e-MBP expressing OLN-93 cells proliferated in low-density cultures (Fig. 5H).

To assess more convincingly a direct correlation between proliferation and nuclear e-MBP expression, we next examined e-MBP localization in low-density cultures in two conditions that inhibit proliferation, i.e., upon serum deprivation, or in the presence of the CDK inhibitor roscovitine (Fig. 6). Concomitant with a 50% block in proliferation in either condition, the percentage of nuclear localization of e-MBP decreased by approx. 50% (Fig. 6A, C). Of note, serum deprivation did not affect the e-MBP expression levels (data not shown). Interestingly, upon re-establishing proliferating conditions (Fig. 6B), i.e., upon addition of serum-containing medium or removal of the CDK inhibitor followed by addition of serum-containing medium, respectively, the level of nuclear e-MBP localization returned to the level at starting conditions.

3.5. shRNA knockdown of MBP in OLN-93 cells decreases proliferation

To determine a direct link between e-MBP and proliferation, a lentiviral-mediated shRNA knockdown of MBP expression in OLN-93 cells was performed. Transduction of OLN-93 cells with shRNA directed against the interface of exon-III and exon-IV, two exons present in all MBP isoforms, showed at an approx. 50% efficiency a significant reduction of e-MBP expression compared to non-transduced cells, as examined by Western blotting (Fig. 7A, approx. 40% reduction) and immunocytochemistry (Fig. 7B). To assess proliferation, a BrdU incorporation assay was combined with GFP immunocytochemistry (Fig. 7C). Proliferation was markedly decreased in GFP-positive cells, i.e., MBP shRNA-containing cells, as compared to GFP-negative cells on the same coverslip (Fig. 7D). Notably, due to the fixation procedure, GFP appeared in the nucleus [45]. Taken together, these data indicate that e-MBP, like postnatal 21.5-kDa MBP, presumably plays a regulatory role in proliferation, which is correlated with its presence in the nucleus. Given its ubiquitous presence in both oligodendroglial cells and non-myelinated tissue [17], we subsequently wondered whether e-MBP may exert its effect beyond that of myelinating cells only, thus reflecting a general role as regulator of cell proliferation.

3.6. e-MBP is also a regulator of proliferation in non-myelinating cell lines

Whereas the postnatal isoforms are exclusively expressed in myelinating cells, e-MBP is present at the protein level in various other tissues during embryonic development, including the liver, thymus, and spleen [17]. However, since the function of e-MBP in other tissues has not been clarified so far, we next explored whether e-MBP may also act as a regulator of proliferation in non-myelinating cells. To this end, three different cell lines, i.e., HEK293 cells, a cell line originally derived from human embryonic kidney, HeLa cells, a human immortal cell line derived from cervical cancer, and HepG2 cells, a human hepatocellular liver carcinoma cell line, were examined by Western blot analysis for e-MBP expression. As shown in Fig. 7E, all examined cell lines express e-MBP, and similarly as observed in OLN-93 cells, e-MBP displayed in all cell lines a nucleocytoplasmic distribution pattern (Fig. 7F). Transduction of HeLa cells with MBP shRNA (approx. 90% efficiency) led to a major reduction in e-MBP expression (Fig. 7G, approx. 90% reduction), with a concomitant decrease in cell proliferation of 50% (Fig. 7H, I). Consistently, cell proliferation was similarly reduced upon downregulation

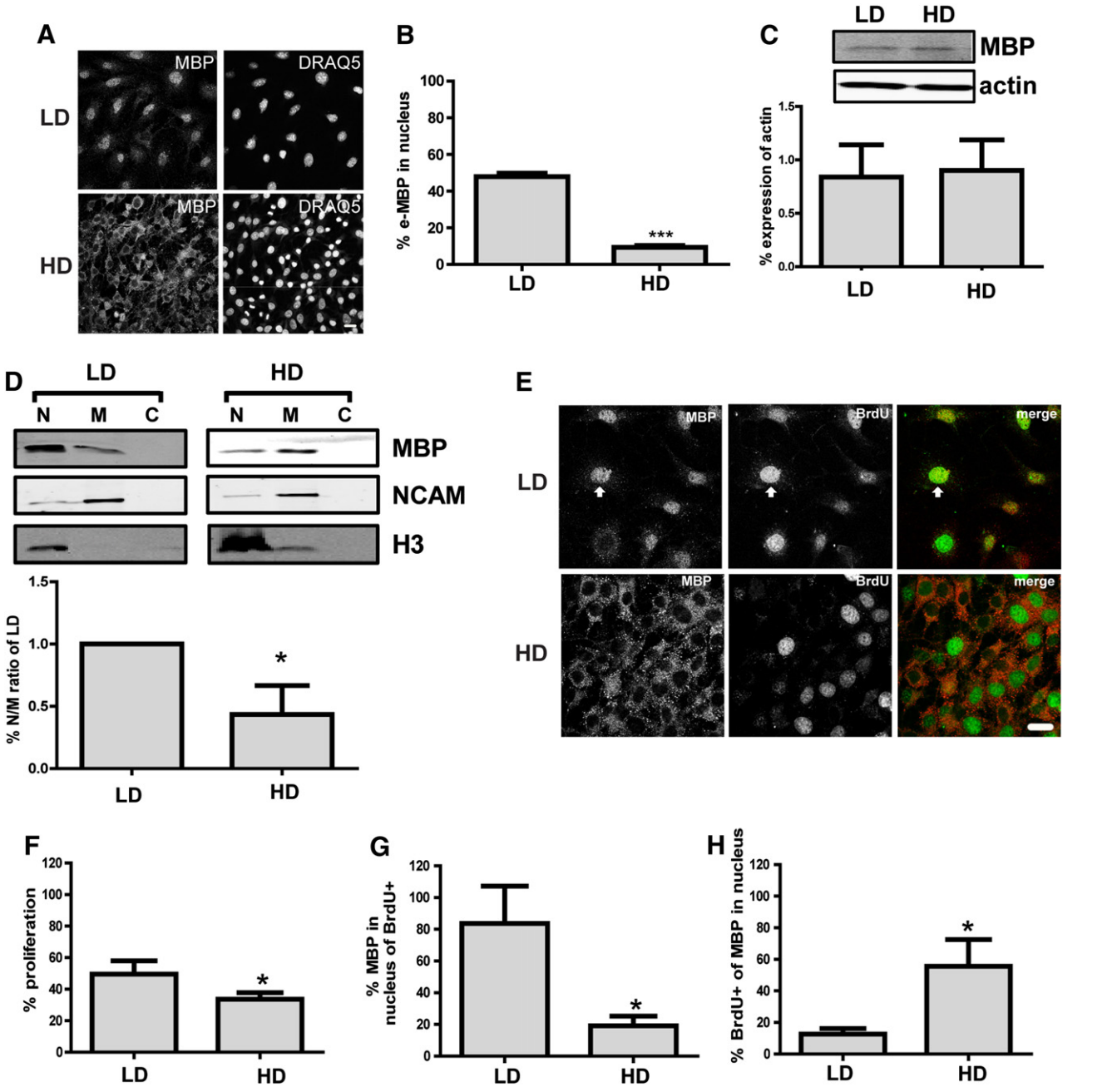

Fig. 5. Cell density dependent localization of e-MBP correlates with cell proliferation. OLN-93 cells were plated at a low density (LD, 2000 cells per well) or high density (HD, 8000 cells per well), and cultured for 3 days. Representative blots and images of at least three independent experiments are shown. (A, B) Cells were fixed and stained for MBP (A). For each condition, the percentage of nuclear e-MBP expression of total DRAQ5-positive cells was determined (B). Note that nuclear e-MBP localization decreased in high cell density cultures. Scale bar is 20 μm. (C) Equal amounts of protein (50 μg) obtained from total OLN-93 cell lysates were subjected to Western blot analysis using the anti-MBP polyclonal antibody. The e-MBP expression levels were quantified relative to the expression of the housekeeping gene β-actin. Note that e-MBP expression levels are similar at both cell densities. (D) OLN-93 cell lysates were subjected to subcellular fractionation followed by Western blot analysis for MBP (pAb), NCAM 140 (membrane marker) and H3 (histone 3, nuclear marker). Equal volumes of nuclear (N), membrane (M), and cytoplasmic (C) fractions were loaded. For each condition, the nucleus to membrane ratio (N/M) of e-MBP was determined taking fraction purity into account. Relative ratio of high-density to low-density cultures is shown, which was set to 1 in each experiment. Note that the nucleus to membrane ratio for e-MBP is decreased in high-density cultures. (E–H) Cell proliferation was determined using a BrdU incorporation assay. The percentage proliferative cells, i.e., BrdU-positive, of total, i.e., DRAQ5-positive cells was determined (F). In panels (E, G) and (H), a BrdU incorporation assay was combined with e-MBP immunocytochemistry. Scale bar in panel E is 20 μM. The percentage of nuclear e-MBP localization in BrdU-positive cells is shown in panel (G) and the percentage of BrdU-positive cells of the nuclear e-MBP containing cells is shown in panel (H). Note that OLN-93 cells proliferate more in low-density cultures, whereas the percentage of proliferating cells with nuclear e-MBP signal is higher in low-density cultures. Statistical analysis in (B–D) and (F–H) was performed using GraphPad Prism 5 [(one-sample) t-test, *$p < 0.05$, ***$p < 0.001$]. Values shown in (B–D) and (F–H) are means + SD of at least three independent experiments.

of e-MBP in HEK293 and HepG2 cells (Supplementary Fig. 4), although to a lesser extent than in OLN-93 and HeLa cells (Fig. 7). Given that at low-density cultures OLN-93 and HeLa cells grow as single cells (Fig. 7), and HepG2 and HEK293 cells in cell clusters with many cell–cell contacts (Supplementary Fig. 4), a partial uncoupling of e-MBP and cell proliferation, for the latter two cell lines could be envisioned, as observed upon cell-cell contact in OLN-93 cells (Fig. 5). Of note, a marked downregulation of e-MBP levels was only observed at least 11 days after transduction with shRNA against MBP, indicating that the turnover of e-MBP is very low and likely cell type dependent.

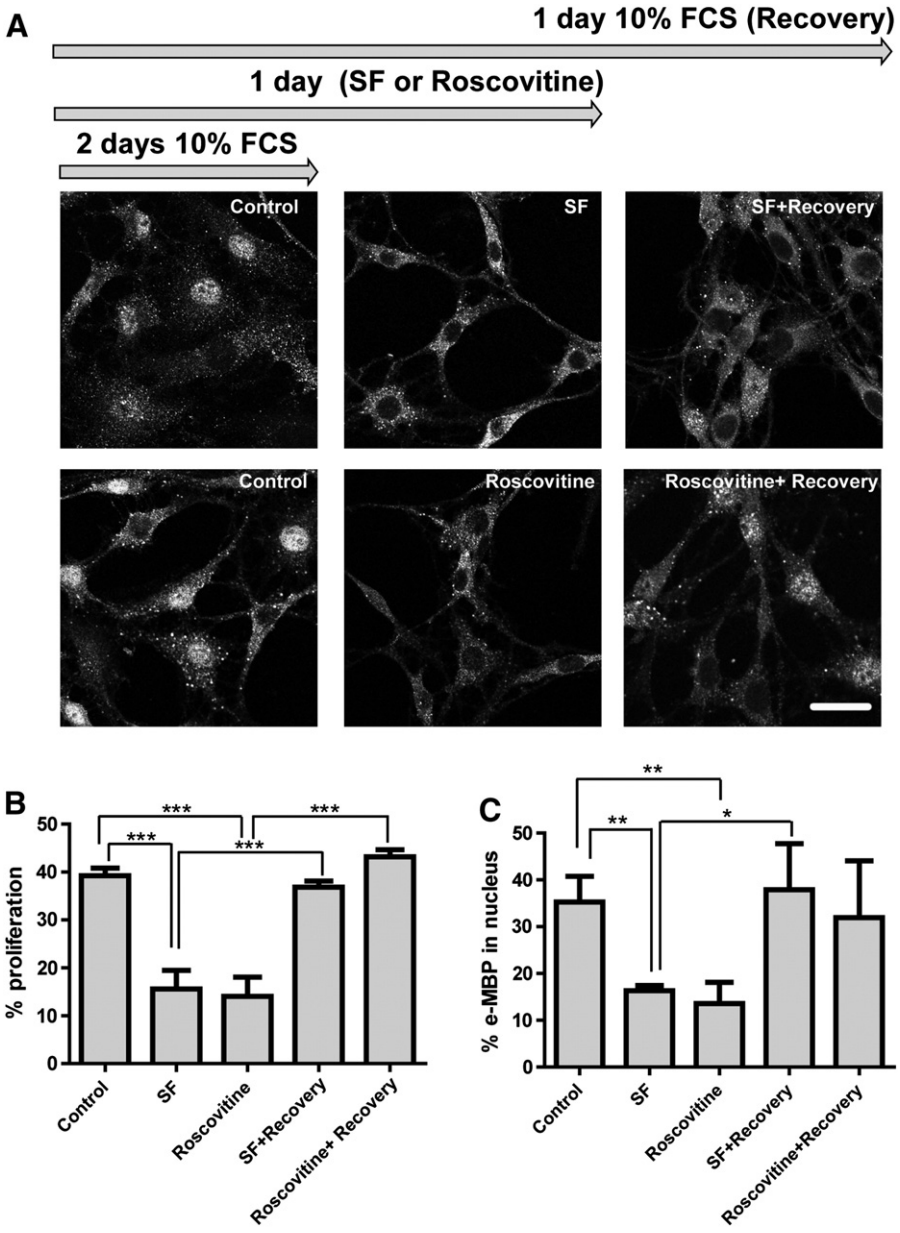

Fig. 6. Localization of e-MBP changes upon mitogenic modulation. OLN-93 cells plated at an initial density of 2000 cells per well were cultured for 2 days, and either fixed (control), or treated with roscovitine (20 μM), or cultured in serum-free (SF) culture medium. After 1 day, cells were fixed or allowed to recover in normal culture medium supplemented with 10% FCS (Recovery) for 1 day. (A) Localization of e-MBP at the indicated conditions, as determined by immunocytochemistry. Representative images of three independent experiments are shown. Scale bar is 20 μm. (B) Cell proliferation as determined with a BrdU incorporation assay. Note that cell proliferation is blocked by 50% when cultured in serum-free (SF) medium or upon treatment with roscovitine, whereas cell proliferation is recovered upon (re)-addition of 10% FCS. (C) Quantitative analysis of (A) at the indicated conditions (the percentage of cells with nuclear e-MBP expression relative to total, DRAQ5-positive cells) was examined. Note that upon inhibition of cell proliferation, e-MBP preferentially localizes to the cytoplasm, whereas in control and during recovery, i.e., at proliferating conditions, e-MBP preferentially localizes to the nucleus. The graphs were plotted as mean + SD and statistical analysis was performed using GraphPad Prism 5 (one-way ANOVA followed by the Newman–Keuls posttest $^{*}p < 0.05$, $^{**}p < 0.01$, $^{***}p < 0.001$).

Taken together, these findings indicate that next to its presence in myelinating cells, e-MBP is also abundantly expressed in embryonic- and cancer-derived cell lines, and appears to act as a general regulator of cell proliferation.

4. Discussion

In the present study, we demonstrate that exon-II-containing embryonic 16-kDa MBP and the postnatal 21.5-kDa MBP shuttle between the nucleus and the cytoplasm, and that their nuclear localization regulates cell proliferation. Thus, in the absence of a mitogenic signal or upon CDK inhibition, the exon-II-containing MBP isoforms translocate from the nucleus to the cytoplasm, and re-appear in the nucleus when proliferation is re-induced. Furthermore, knockdown of MBP via shRNA interference significantly decreased proliferation. Therefore, exon-II-containing MBPs might be prominent regulators of oligodendrocyte proliferation. In this context, given the increased expression of postnatal exon-II-positive MBP isoforms at the onset of remyelination [16,46], it is tempting to suggest that these isoforms might function in a similar manner as important mediators in the early regulation of myelin biogenesis.

Classical MBP isoforms are generally considered as important markers for differentiated oligodendrocytes because of their localization and functioning in the myelin sheath. However, these different MBP isoforms are generated upon alternative splicing of a single MBP transcript of three of its seven exons, i.e., exons II, V, and VI. Specifically, the

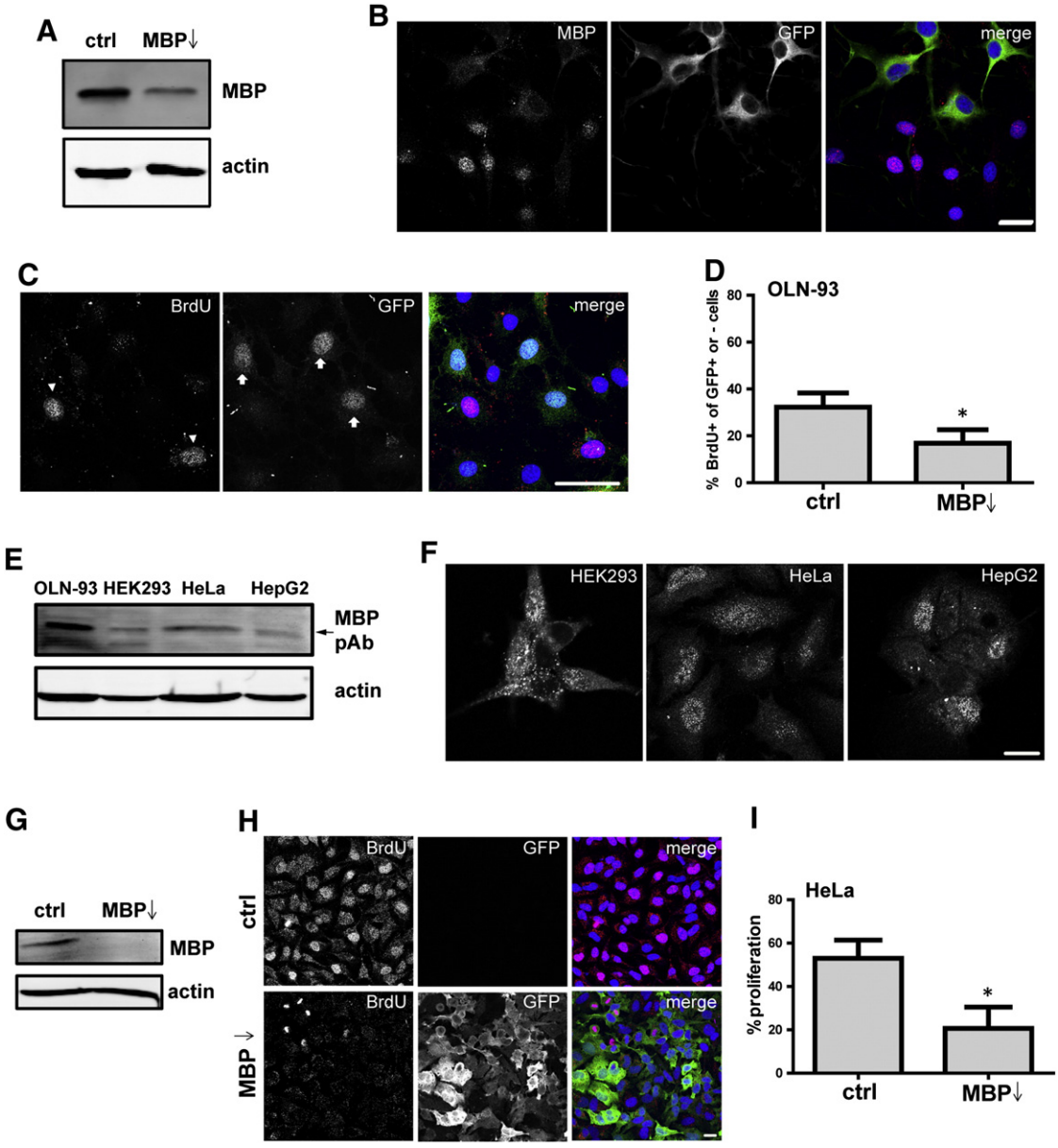

Fig. 7. shRNA knockdown of MBP significantly decreases cell proliferation. (A–D) OLN-93 cells were untreated (ctrl), or transduced with shRNA directed against all isoforms of MBP (MBP ↓), and analyzed 12 days after transduction. (A) Equal amounts of protein (20 μg) were subjected to Western blot analysis using the anti-MBP polyclonal antibody. Note the significant reduction (40%) of e-MBP protein upon transduction with MBP shRNA. (B) Cells were fixed and co-stained for MBP and GFP. The expression of GFP confirms the shRNA lentiviral transduction. A representative confocal image of three independent experiments is shown. Scale bar is 20 μm. Note that e-MBP is absent in GFP-positive cells. (C–D) Cell proliferation was determined using a BrdU incorporation assay combined with GFP immunocytochemistry (C). Scale bar is 20 μm. The percentage of proliferative cells, i.e., BrdU-positive (arrowhead), of total GFP-positive (arrow) and GFP-negative cells (ctrl) was determined (D). Note that OLN-93 cells that contain shRNA against MBP, i.e., GFP-positive cells, proliferate less. Statistical analysis in (D) was performed using GraphPad Prism 5 (t-test, $^*p < 0.05$). Values shown in panel (D) are means + SD of at least three independent experiments. (E) Equal amounts of protein (50 μg) were subjected to Western blot analysis using the anti-MBP polyclonal antibody. Note the presence of e-MBP in the examined cell lines (arrow). (F) The indicated cell lines were fixed at 24 h in culture and stained with anti-MBP monoclonal antibody. A representative confocal image of three independent experiments is shown. Note that MBP localizes both to the nucleus (bright fluorescence) and to the cytoplasm (punctate appearance) in the examined cell lines. Scale bar is 20 μm. (G–I) HeLa cells were untreated (ctrl), or transduced with shRNA directed against all isoforms of MBP (MBP↓), and analyzed 12 days after transduction. (G) Equal amounts of protein (70 μg) were subjected to Western blot analysis using the anti-MBP polyclonal antibody. Note the significant reduction (90%) of e-MBP protein upon transduction with MBP shRNA. (H, I) Cell proliferation was determined using a BrdU incorporation assay combined with GFP immunocytochemistry (H). Scale bar is 20 μm. The percentage of proliferative cells, i.e., BrdU-positive, of total cells was determined (I). Note that HeLa cells that contain shRNA against MBP, i.e., GFP-positive cells, proliferate less. Statistical analysis in panel I was performed using GraphPad Prism 5 (t-test, $^*p < 0.05$). Values shown in panel I are means + SD of at least three independent experiments.

expression of exon-V-negative MBP isoforms is apparent already at embryonic development, and their subsequent (dis)appearance at the postnatal stage is developmentally regulated [16,17], emphasizing their distinct roles throughout the development of myelinating cells. Here, we show that the oligodendrocyte progenitor cell line, OLN-93, expresses an exon-II-positive embryonic 16-kDa MBP isoform, which is localized to the nucleus and cytoplasm. The subcellular localization of e-MBP is regulated by cell–cell interactions, i.e., e-MBP redistributed to the cytoplasm at high cell density, like classical postnatal exon-II-containing MBP isoforms [12,24]. As observed for many cell types, and consistent with a density-dependent diminution of the proliferation of OPCs [47,48], OLN-93 cell proliferation was markedly decreased upon cell–cell contact. At low cell density, the majority of the proliferating cells showed a nuclear localization of e-MBP, suggesting a role for nucleus localized e-MBP in cell proliferation. However, in the absence of a mitogenic signal, e-MBP translocated from the nucleus to the cytoplasm,

yet re-appeared in the nucleus when proliferation was re-induced. Notably, in the low-density cultures, the majority of OLN-93 cells that had nuclear e-MBP did not proliferate during an 8 h BrdU pulse, suggesting that nuclear e-MBP as such regulates rather than triggers proliferation. Indeed, at high cell density, OLN-93 cells with e-MBP localized in the cytoplasm were still remarkably proliferative, whereas cells in these cultures with fewer cell–cell contacts showed nuclear e-MBP localization and proliferated. The latter phenomenon presumably reflects the same process as observed at low cell density. In addition, knock-down of MBP gene expression via RNA interference confirmed a role for e-MBP in proliferation at low cell density. Hence, our data indicate that nuclear-localized e-MBP likely regulates cell proliferation upon mitogenic activation, i.e., in the absence of cell–cell contact, whereas upon cell–cell interactions, an e-MBP independent proliferation signaling pathway might be activated [49].

Here, we also demonstrate that the expression and function of e-MBP is not restricted to cells of the oligodendrocyte lineage. Thus, e-MBP is also expressed in several non-CNS cell lines showing a nucleocytoplasmic distribution pattern, while its downregulation by shRNA resulted in a decrease of cell proliferation. Therefore, e-MBP appears to play a role in proliferation in a variety of tissues during embryonic and neonatal development. In addition, given the expression of e-MBP in cancer-derived cell lines, a role in the proliferation of cancer cells might be envisioned. However, and similar to OLN-93 cells, a partial uncoupling of e-MBP and cell proliferation was observed in cell lines with many cell–cell contacts. These findings also imply that e-MBP does not require oligodendrocyte specific factors for regulating proliferation. Although the mechanism by which e-MBP regulates cell proliferation is not known at this time, our preliminary work suggests a direct interaction between e-MBP and the well-known and ubiquitous CDK inhibitor p27 under proliferating conditions, whereas live-cell imaging studies demonstrated that e-MBP exits the nucleus before p27 (our unpublished observations).

During postnatal development, the level of expression of MBP isoforms is markedly modulated in oligodendrocytes and not in the other tissues. The appearance of postnatal MBP isoforms is regulated at the transcription level via a coordinated action of various oligodendrocyte-specific transcription factors [50,51]. Thus, the level of e-MBP decreases rapidly (Fig. 4), while postnatal exon-II-containing MBP isoforms peak during early development [14]. In contrast, the exon-II-negative postnatal isoforms are primarily expressed at later stages of oligodendrocyte maturation [2,11,12,14,16]. As for exon-II-containing e-MBP, the nuclear localization of postnatal exon-II-containing 21.5-kDa MBP–RFP correlated with increased proliferation. Quantitative FRAP analysis revealed that the nuclear import rate of 21.5-kDa MBP–RFP decreased upon serum deprivation, whereas concomitantly, the nuclear export rate increased. Replenishment of serum, i.e., activating proliferation, restored the nuclear import rate to a similar level as observed before serum deprivation. Interestingly, re-establishment of the nuclear export rate displayed a lag phase, which might suggest that modifications of 21.5-kDa MBP–RFP might be essential for its nuclear export. Indeed, phosphorylation of many nuclear-localized proteins, e.g., p27, has been associated with their nuclear export [33,52], as has also been suggested for 21.5-kDa MBP export [24]. Nuclear MBP isoforms do carry two non-traditional PY-nuclear localization signals within the exon-II sequence [53], whereas they do not possess a classical nuclear export signal. The nuclear export of MBP apparently requires another protein, since our live-cell imaging data and FRAP analysis revealed that the CRM1 nuclear export inhibitor, LMB, prevented nuclear export of 21.5-kDa MBP–RFP.

Taken together, in contrast to exon-II devoid MBP isoforms that act as a molecular sieve and have a role in myelin compaction [2,19,22], postnatal and embryonic exon-II-containing MBP isoforms likely play a regulatory role in oligodendrocyte proliferation. The exact role of 26 amino acids containing exon-II in this process remains to be determined, particularly since very recently golli MBPs, which lack exon-II [54] may also show a nuclear localization pattern, and have been proposed to play a role in oligodendrocyte proliferation during remyelination [55]. Further studies are needed to reveal the underlying mechanism(s) as to how e-MBP and postnatal exon-II-positive MBP modulate proliferation, and whether these mechanisms are similar. As shown in the present manuscript in OLN-93 cells, and in a previous study in N19 cells [27], the proliferation of both transfected *and* untransfected cells was increased, while a nuclear localization of 21.5-kDa MBP–RFP was required. Therefore, expression of exon-II-containing MBPs highly likely increased cell proliferation via a diffusible factor, and although the identity of this diffusible factor is currently unknown, the expression and/or secretion might be regulated by the presence of exon-II-containing MBP in the nucleus or its absence in the cytoplasm. Given that e-MBP is functionally expressed in other tissues [17,41] and in a variety of cell lines (as we have shown here), an understanding of the mechanism(s) might also provide novel means to control (ab)normal proliferation, as occurs in cancer.

Acknowledgements

The authors thank Dr. Joan Boggs for critically reading the manuscript, Dr. Liliana Pedraza for her kind gift of anti-exon-II MBP antibody, and Klaas Sjollema for excellent technical assistance with the live-cell imaging and FRAP experiments. This work was supported by grants from the Netherlands Foundation for the Support of MS Research ('Stichting MS Research') and the Netherlands Organization of Scientific Research NWO (VIDI and Aspasia, to W.B.). GSTS was the recipient of a Doctoral Studentship from the Multiple Sclerosis Society of Canada. The work in the Guelph laboratory was supported initially by the Canadian Institutes of Health Research (MOP #86483 to Joan Boggs and GH) and presently by the Natural Sciences and Engineering Research Council of Canada (RG121541 to GH). Part of the work has been performed at the UMCG Microscopy and Imaging Center (UMIC), which is sponsored by NWO grants 40-00506-98-9021 and 175-010-2009-023.

Appendix A. Supplementary data

Supplementary data to this article can be found online at http://dx.doi.org/10.1016/j.bbamcr.2013.11.026.

References

[1] N. Baumann, D. Pham-Dinh, Biology of oligodendrocyte and myelin in the mammalian central nervous system, Physiol. Rev. 81 (2001) 871–927.
[2] J.M. Boggs, Myelin basic protein: a multifunctional protein, Cell. Mol. Life Sci. 63 (2006) 1945–1961.
[3] G.F. Chernoff, Shiverer: an autosomal recessive mutant mouse with myelin deficiency, J. Hered. 72 (1981) 128.
[4] G. Harauz, J.M. Boggs, Myelin management by the 18.5-kDa and 21.5-kDa classic myelin basic protein isoforms, J. Neurochem. 125 (2013) 334–361.
[5] C. Readhead, L. Hood, The dysmyelinating mouse mutations shiverer (shi) and myelin deficient (shimld), Behav. Genet. 20 (1990) 213–234.
[6] A.T. Campagnoni, T.M. Pribyl, C.W. Campagnoni, K. Kampf, S. Amur-Umarjee, C.F. Landry, et al., Structure and developmental regulation of Golli-mbp, a 105-kilobase gene that encompasses the myelin basic protein gene and is expressed in cells in the oligodendrocyte lineage in the brain, J. Biol. Chem. 268 (1993) 4930–4938.
[7] M.I. Givogri, E.R. Bongarzone, V. Schonmann, A.T. Campagnoni, Expression and regulation of golli products of myelin basic protein gene during in vitro development of oligodendrocytes, J. Neurosci. Res. 66 (2001) 679–690.
[8] M.C. Marty, F. Alliot, J. Rutin, R. Fritz, D. Trisler, B. Pessac, The myelin basic protein gene is expressed in differentiated blood cell lineages and in hemopoietic progenitors, Proc. Natl. Acad. Sci. U. S. A. 99 (2002) 8856–8861.
[9] T.M. Pribyl, C.W. Campagnoni, K. Kampf, T. Kashima, V.W. Handley, J. McMahon, et al., The human myelin basic protein gene is included within a 179-kilobase transcription unit: expression in the immune and central nervous systems, Proc. Natl. Acad. Sci. U. S. A. 90 (1993) 10695–10699.
[10] A.T. Campagnoni, Molecular biology of myelin proteins from the central nervous system, J. Neurochem. 51 (1988) 1–14.
[11] H. de Vries, J.C. de Jonge, C. Schrage, M.E. van der Haar, D. Hoekstra, Differential and cell development-dependent localization of myelin mRNAs in oligodendrocytes, J. Neurosci. Res. 47 (1997) 479–488.

[12] L. Pedraza, L. Fidler, S.M. Staugaitis, D.R. Colman, The active transport of myelin basic protein into the nucleus suggests a regulatory role in myelination, Neuron 18 (1997) 579–589.
[13] S.M. Staugaitis, P.R. Smith, D.R. Colman, Expression of myelin basic protein isoforms in nonglial cells, J. Cell Biol. 110 (1990) 1719–1727.
[14] E. Barbarese, J.H. Carson, P.E. Braun, Accumulation of the four myelin basic proteins in mouse brain during development, J. Neurochem. 31 (1978) 779–782.
[15] J.H. Carson, M.L. Nielson, E. Barbarese, Developmental regulation of myelin basic protein expression in mouse brain, Dev. Biol. 96 (1983) 485–492.
[16] G.M. Kruger, L.T. Diemel, C.A. Copelman, M.L. Cuzner, Myelin basic protein isoforms in myelinating and remyelinating rat brain aggregate cultures, J. Neurosci. Res. 56 (1999) 241–247.
[17] P.M. Mathisen, S. Pease, J. Garvey, L. Hood, C. Readhead, Identification of an embryonic isoform of myelin basic protein that is expressed widely in the mouse embryo, Proc. Natl. Acad. Sci. U. S. A. 90 (1993) 10125–10129.
[18] K. Nakajima, K. Ikenaka, T. Kagawa, J. Aruga, J. Nakao, K. Nakahira, et al., Novel isoforms of mouse myelin basic protein predominantly expressed in embryonic stage, J. Neurochem. 60 (1993) 1554–1563.
[19] S. Aggarwal, L. Yurlova, N. Snaidero, C. Reetz, S. Frey, J. Zimmermann, et al., A size barrier limits protein diffusion at the cell surface to generate lipid-rich myelin-membrane sheets, Dev. Cell 21 (2011) 445–456.
[20] D. Fitzner, A. Schneider, A. Kippert, W. Mobius, K.I. Willig, S.W. Hell, et al., Myelin basic protein-dependent plasma membrane reorganization in the formation of myelin, EMBO J. 25 (2006) 5037–5048.
[21] M. Simons, N. Snaidero, S. Aggarwal, Cell polarity in myelinating glia: from membrane flow to diffusion barriers, Biochim. Biophys. Acta 1821 (2012) 1146–1153.
[22] G. Harauz, V. Ladizhansky, J.M. Boggs, Structural polymorphism and multifunctionality of myelin basic protein, Biochemistry 48 (2009) 8094–8104.
[23] G.S.T. Smith, P.M. Paez, V. Spreuer, C.W. Campagnoni, J.M. Boggs, A.T. Campagnoni, et al., Classical 18.5-and 21.5-kDa isoforms of myelin basic protein inhibit calcium influx into oligodendroglial cells, in contrast to golli isoforms, J. Neurosci. Res. 89 (2011) 467–480.
[24] G.S.T. Smith, M. De Avila, P.M. Paez, V. Spreuer, M.K.B. Wills, N. Jones, et al., Proline substitutions and threonine pseudophosphorylation of the SH3 ligand of 18.5-kDa myelin basic protein decrease its affinity for the Fyn-SH3 domain and alter process development and protein localization in oligodendrocytes, J. Neurosci. Res. 90 (2012) 28–47.
[25] G.S.T. Smith, L. Homchaudhuri, J.M. Boggs, G. Harauz, Classic 18.5- and 21.5-kDa myelin basic protein isoforms associate with cytoskeletal and SH3-domain proteins in the immortalized N19-oligodendroglial cell line stimulated by phorbol ester and IGF-1, Neurochem. Res. 37 (2012) 1277–1295.
[26] L. Pedraza, Nuclear transport of myelin basic protein, J. Neurosci. Res. 50 (1997) 258–264.
[27] G.S.T. Smith, B. Samborska, S.P. Hawley, J.M. Klaiman, T.E. Gillis, N. Jones, et al., Nucleus-localized 21.5-kDa myelin basic protein promotes oligodendrocyte proliferation and enhances neurite outgrowth in coculture, unlike the plasma membrane-associated 18.5-kDa isoform, J. Neurosci. Res. 91 (2013) 349–362.
[28] O. Maier, T. van der Heide, A.-M. van Dam, W. Baron, H. de Vries, D. Hoekstra, Alteration of the extracellular matrix interferes with raft association of neurofascin in oligodendrocytes. Potential significance for multiple sclerosis? Mol. Cell. Neurosci. 28 (2005) 390–401.
[29] C. Richter-Landsberg, M. Heinrich, OLN-93: a new permanent oligodendroglia cell line derived from primary rat brain glial cultures, J. Neurosci. Res. 45 (1996) 161–173.
[30] M. Stancic, D. Slijepcevic, A. Nomden, M.J. Vos, J.C. de Jonge, A.H. Sikkema, et al., Galectin-4, a novel neuronal regulator of myelination, Glia 60 (2012) 919–935.
[31] B. Klunder, W. Baron, C. Schrage, J. de Jonge, H. de Vries, D. Hoekstra, Sorting signals and regulation of cognate basolateral trafficking in myelin biogenesis, J. Neurosci. Res. 86 (2008) 1007–1016.
[32] M. Sharma, C. Jamieson, M. Johnson, M.P. Molloy, B.R. Henderson, Specific armadillo repeat sequences facilitate β-catenin nuclear transport in live cells via direct binding to nucleoporins Nup62, Nup153, and RanBP2/Nup358, J. Biol. Chem. 287 (2012) 819–831.
[33] N. Ishida, T. Hara, T. Kamura, M. Yoshida, K. Nakayama, K.I. Nakayama, Phosphorylation of p27Kip1 on serine 10 is required for its binding to CRM1 and nuclear export, J. Biol. Chem. 277 (2002) 14355–14358.
[34] B.-C. Jang, U. Muñoz-Najar, J.-H. Paik, K. Claffey, M. Yoshida, T. Hla, Leptomycin B, an inhibitor of the nuclear export receptor CRM1, inhibits COX-2 expression, J. Biol. Chem. 278 (2003) 2773–2776.
[35] D. Axelrod, D.E. Koppel, J. Schlessinger, E. Elson, W.W. Webb, Mobility measurement by analysis of fluorescence photobleaching recovery kinetics, Biophys. J. 16 (1976) 1055–1069.
[36] V. Cimica, H.-C. Chen, J.K. Iyer, N.C. Reich, Dynamics of the STAT3 transcription factor: nuclear import dependent on Ran and importin-β1, PLoS ONE 6 (2011) e20188.
[37] K. Jacobson, E. Wu, G. Poste, Measurement of the translational mobility of concanavalin A in glycerol–saline solutions and on the cell surface by fluorescence recovery after photobleaching, Biochim. Biophys. Acta 433 (1976) 215–222.
[38] E. Krieghoff, J. Behrens, B. Mayr, Nucleo-cytoplasmic distribution of beta-catenin is regulated by retention, J. Cell Sci. 119 (2006) 1453–1463.
[39] F.M. Townsley, A. Cliffe, M. Bienz, Pygopus and Legless target Armadillo/β-catenin to the nucleus to enable its transcriptional co-activator function, Nat. Cell Biol. 6 (2004) 626–633.
[40] K.L. Sunn, J.A. Eisman, E.M. Gardiner, D.A. Jans, FRAP analysis of nucleocytoplasmic dynamics of the vitamin D receptor splice variant VDRB1: preferential targeting to nuclear speckles, Biochem. J. 388 (2005) 509–514.
[41] J.A. Määttä, E.T. Coffey, J.A. Hermonen, A.A. Salmi, A.E. Hinkkanen, Detection of myelin basic protein isoforms by organic concentration, Biochem. Biophys. Res. Commun. 238 (1997) 498–502.
[42] R.J. Hardy, R.A. Lazzarini, D.R. Colman, V.L. Friedrich, Cytoplasmic and nuclear localization of myelin basic proteins reveals heterogeneity among oligodendrocytes, J. Neurosci. Res. 46 (1996) 246–257.
[43] I. Kokkinopoulos, G. Shahabi, A. Colman, G. Jeffery, Mature peripheral RPE cells have an intrinsic capacity to proliferate; a potential regulatory mechanism for age-related cell loss, PLoS ONE 6 (2011) e18921.
[44] M.E. Warchol, Cell density and N-cadherin interactions regulate cell proliferation in the sensory epithelia of the inner ear, J. Neurosci. 22 (2002) 2607–2616.
[45] U. Schnell, F. Dijk, K.A. Sjollema, B.N.G. Giepmans, Immunolabeling artifacts and the need for live-cell imaging, Nat. Methods 9 (2012) 152–158.
[46] C.A. Jordan, V.L. Friedrich Jr., F. de Ferra, D.G. Weismiller, K.V. Holmes, M. Dubois-Dalcq, Differential exon expression in myelin basic protein transcripts during central nervous system (CNS) remyelination, Cell. Mol. Neurobiol. 10 (1990) 3–18.
[47] Y. Nakatsuji, R.H. Miller, Control of oligodendrocyte precursor proliferation mediated by density-dependent cell cycle protein expression, Dev. Neurosci. 23 (2001) 356–363.
[48] H. Zhang, R.H. Miller, Density-dependent feedback inhibition of oligodendrocyte precursor expansion, J. Neurosci. 16 (1996) 6886–6895.
[49] C.M. Nelson, C.S. Chen, Cell–cell signaling by direct contact increases cell proliferation via a PI3K-dependent signal, FEBS Lett. 514 (2002) 238–242.
[50] B. Emery, D. Agalliu, J.D. Cahoy, T.A. Watkins, J.C. Dugas, S.B. Mulinyawe, et al., Myelin gene regulatory factor is a critical transcriptional regulator required for CNS myelination, Cell 138 (2009) 172–185.
[51] Q. Wei, W.K. Miskimins, R. Miskimins, Stage-specific expression of myelin basic protein in oligodendrocytes involves Nkx2.2-mediated repression that is relieved by the Sp1 transcription factor, J. Biol. Chem. 280 (2005) 16284–16294.
[52] G. Rodier, A. Montagnoli, L. Di Marcotullio, P. Coulombe, G.F. Draetta, M. Pagano, et al., p27 cytoplasmic localization is regulated by phosphorylation on Ser10 and is not a prerequisite for its proteolysis, EMBO J. 20 (2001) 6672–6682.
[53] G.S.T. Smith, L.V. Seymour, J.M. Boggs, G. Harauz, The 21.5-kDa isoform of myelin basic protein has a non-traditional PY-nuclear-localization signal, Biochem. Biophys. Res. Commun. 422 (2012) 670–675.
[54] J.-M. Feng, Minireview: expression and function of golli protein in immune system, Neurochem. Res. 32 (2007) 273–278.
[55] P.M. Paez, V.T. Cheli, C.A. Ghiani, V. Spreuer, V.W. Handley, A.T. Campagnoni, Golli myelin basic proteins stimulate oligodendrocyte progenitor cell proliferation and differentiation in remyelinating adult mouse brain, Glia 60 (2012) 1078–1093.